Alignment Control of Carbon Nanotube Forest from Random to Nearly Perfectly Aligned by Utilizing the Crowding Effect

Ming Xu,[†,‡] Don N. Futaba,[†,‡,*] Motoo Yumura,[†,‡] and Kenji Hata[†,‡,§,*]

[†]Technology Research Association for Single Wall Carbon Nanotubes (TASC), Tsukuba, 305-8565, Japan, [‡]Nanotube Research Center, National Institute of Advanced Industrial Science and Technology (AIST), Tsukuba, 305-8565, Japan, and [§]Japan Science and Technology Agency (JST), Kawaguchi, 332-0012, Japan

ABSTRACT Alignment represents an important structural parameter of carbon nanotubes (CNTs) owing to their exceptionally high aspect ratio, one-dimensional property. In this paper, we demonstrate a general approach to control the alignment of few-walled CNT forests from nearly random to nearly ideally aligned by tailoring the density of active catalysts at the catalyst formation stage, which can be experimentally achieved by controlling the CNT forest mass density. Experimentally, we found that the catalyst density and the degree of alignment were inseparably linked because of a crowding effect from neighboring CNTs, that is, the increasing confinement of CNTs with increased density. Therefore, the CNT density governed the degree of alignment, which increased monotonically with the density. This relationship, in turn, allowed the precise control of the alignment through control of the mass density. To understand this behavior further, we developed a simple, first-order model based on the flexural modulus of the CNTs that could quantitatively describe the relationship between the degree of alignment (HOF) and carbon nanotube spacing (crowding effect) of any type of CNTs.

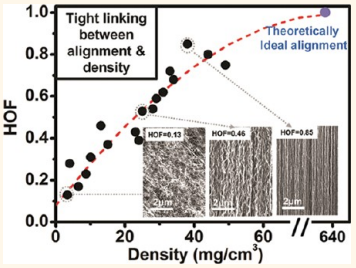

KEYWORDS: carbon nanotubes · cnt · forest · alignment · crowding effect · catalyst · density

Alignment represents an important structure parameter of bulk solid materials, particularly for one-dimensional (1-D) materials with high aspect ratio, such as polymer chains, fibers and proteins, because alignment describes the degree of the order of the components within the bulk. From a structural standpoint, high alignment is analogous with a crystalline (or highly ordered) phase, while, in contrast, low alignment represents an isotropic or amorphous phase. In highly ordered materials composed of aligned one-dimensional components, dense packing minimizes lateral freedom within the bulk. Therefore, the material would exhibit similar anisotropic properties of the individual components from the mutual reinforcement along the alignment axis. Hence, in general, such materials tend to be strong, rigid, and brittle, such as yarns, liquid crystals, and composites from aligned fibers/polymers.[1,2] In contrast, a disordered material made from nonaligned (randomly oriented) one-dimensional components would be more loosely packed and possess more internal degrees of freedom, and thus in general, would exhibit more compliance, flexibility, and ductility. Apt examples are nonwoven fabrics made from nonaligned fibers,[3] such as felts, paper, *etc.*

As exemplified, due to the impact of alignment on properties, when constructing materials, tailoring the degree of alignment of the components is of fundamental importance. For example, plastic drink bottles are composed entirely of polyethylene (PE) but with different alignment degrees for different parts (*i.e.*, hard cap and flexible bottle). PE with 45−55% crystallinity percentage possesses lower strength (10 MPa) and higher resilience, which is used for the bottle itself. With increased crystallinity percentage (70%), that is, higher alignment degree among polymer chains, the material becomes more brittle and two-times stiffer, and can therefore be used for bottle cap. For polymer materials, control of the alignment degree, that is, crystallinity percentage, can be achieved by annealing, stretching, and solvent selection.[4]

As being a one-dimensional material possessing the highest aspect ratio, carbon nanotubes (CNTs) follow a similar scheme, and therefore intense effort has been conducted to fabricate either aligned or nonaligned CNT

* Address correspondence to kenji-hata@aist.go.jp, d-futaba@aist.go.jp.

Received for review January 12, 2012 and accepted June 17, 2012.

Published online June 18, 2012
10.1021/nn300142j

materials. For example, aligned CNTs have been assembled into fibers exhibiting tensile strength stronger than those of carbon fibers.[5] In addition, aligned CNTs have demonstrated as fillers to make the epoxy composites with the highest reported Young's modulus.[6] In contrast, nonaligned CNTs have been "assembled" into nonwoven films,[7] such as buckypapers[8] and CNT sponges[9] that have demonstrated both flexibility and robustness. Through these researches, alignment control of CNTs through post-treatment methods has been recognized as being difficult, such as dispersion, solidification, and mechanical densification,[10−12] because CNTs are extremely long and easily aggregate and entangle by the strong van der Waals (vdW) interaction.

Therefore, it would be a great advantage to control the degree of alignment of the bulk CNT material at the synthesis stage. Synthetic control would facilitate further processing steps to achieve the desired degree of alignment of the CNTs in the final product. From this standpoint, a promising approach is to use the self-assembly effect during growth to synthesize aligned and nonaligned CNTs materials. A well-established example is vertically aligned CNTs (forests) grown from catalysts on a substrate. Here, the CNTs spontaneously align during growth without any external processing, and thus it is possible to align even very long CNTs. The aligned CNT forest has demonstrated advantages for strain sensors,[13] prepregs for epoxy/CNT composite sheets,[14] supercapacitor electrodes,[10] and electrical interconnects for large scale integration vias.[15] Recently, the synthetic control of nonaligned CNT macroscopic structures has been demonstrated, such as the CNT sponge and nonaligned CNT forests.[9,16] Such nonaligned forests showed temperature-invariant rubber-like viscoelasticity over a wide range of temperature from −196 °C to ∼1000 °C.[16] This behavior is exclusive to nonaligned forests, exemplifying the strong influence of alignment on the physical properties of CNT materials. Despite the importance, previous reports on alignment control have only showed a "digital" control, that is, aligned or nonaligned, and there have been no reports demonstrating an approach to precisely control the degree of alignment over a wide range in an "analog" manner.

In this paper, we address this issue and propose a fundamental approach to synthesize CNT forests on substrates with a precise and continuous control of degree of alignment from nearly random to almost ideally aligned (Herman's Orientation Factor (HOF) values ranging from 0.13 to 0.85 with resolution of 0.05). We found that the alignment was tightly linked to the CNT density stemming from the crowding effect from neighboring CNTs, that is, the increasing confinement among CNTs with increased density. From these experimental results, we have proposed a simple, quantitative model based on the flexural modulus of the CNTs that could describe the relationship between the degree of alignment (HOF) and carbon nanotube spacing (crowding effect) of any type of CNTs.

RESULTS AND DISCUSSION

First, we begin by demonstrating the alignment control of CNT forests (Figure 1a) over a wide range with high precision by a series of cross-sectional scanning electron microscope (SEM) images (Figure 1b) of millimeter length scale CNT forests. SEM images show the progression of alignment from laterally traversing CNTs without any preferred direction, to a gradual increase in vertical orientation, to obvious vertical alignment with little observable lateral traversing. These CNT forests were grown by the water-assisted chemical vapor deposition (CVD) technique,[17] with ethylene as the carbon source and water as the growth enhancer. Alignment control was achieved by tailoring the catalyst density as described later. Hence, the growth conditions were identical, and this point was important to solely change the degree of alignment while not altering other structural parameters, such as diameter (3−5.5 nm) and wall number (1−2) (detailed synthesis conditions are shown in Supporting Information, Table 1). Also importantly, we did not sacrifice the yield to extend our range of alignment control and could easily grow CNT forests (Figure 1) with heights exceeding 1 mm in 10 min over the entire range. Characterization of the CNTs by transmission electron microscopy (TEM) showed only small variance in average diameter (∼4 nm) and wall number (∼two walls) among samples confirming that alignment was controlled without influencing other structural parameters (TEM images are in Supporting Information, Figure S1).

Our results were compared to other relevant studies. The highest level of alignment achieved was comparable to the "super-aligned" forests reported by Jiang *et al.*[18,19] and Baughman *et al.*[20] that were useful for spinning yarns and sheets. In contrast, the CNT sponges reported by Cao *et al.*[9] and the CNT cotton by Ajayan *et al.*[21] are likely to be less aligned than the nonaligned forests achieved here, because they were made from CNT synthesized by a floating catalyst CVD method deposited on a substrate and therefore not grown directly from catalysts on a substrate. Furthermore, there have been reports of "digital" control of alignment of CNT forests, that is, aligned or nonaligned, through the control in catalyst thin film thickness, but associated with this alignment difference was a stark change in wall number (2−25 walls) and yield (2.2 mm to 0.38 mm), meaning that the change in the alignment likely stemmed from the change in the CNT structure.[22] Another report of digital control was by Robertson *et al.* who synthesized aligned and nonaligned forests by changing the annealing gas from He/H_2 to O_2.[23] Herman's Orientation Factor (HOF) was used to quantify the degree of alignment where 0 and 1 represents random and perfect alignment,

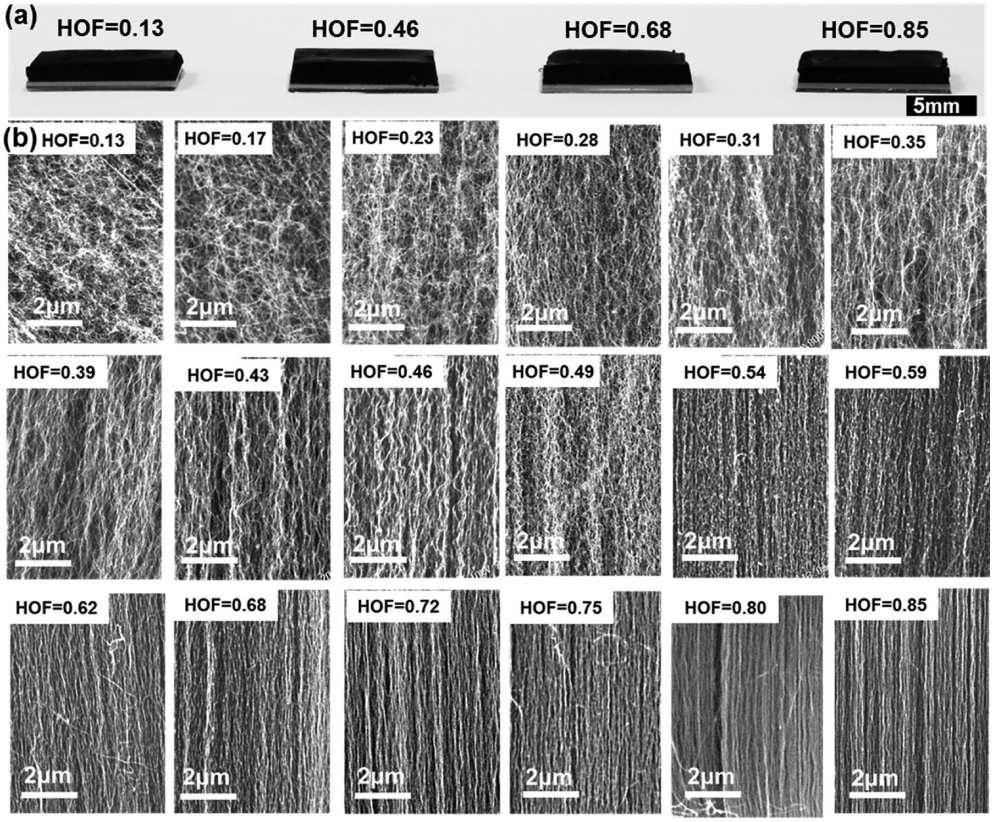

Figure 1. Demonstration of precise alignment control nearly spanning the full range of random to nearly perfect alignment. (a) Photograghs of the CNT forest with the heights of ~1 mm at different degrees of alignment. (b) Scanning electron microscopy images showing the wide range of alignment with the HOFs ranged from 0.13 to 0.85.

respectively.[24,25] Following the procedures described later, the HOF was calculated from fast Fourier transforms (FFT) of the cross-sectional SEM images and showed the controllable range of alignment to be from 0.13 to 0.85 with the resolution less than 0.05. These limits correspond to an ideally aligned sample with an alignment variance of 77° and 5°, respectively.

We would like to note that the fundamental mechanism that provided us an approach to allow control of alignment. Importantly, when the HOF was plotted as a function of the CNT forest density, we found that they were nearly linearly related (Figure 2), and all the experimental data fell on a narrow linear region with no points in the regions above or below.

Associated with a one-order increase in density from 3.3 to 44 mg/cm^3, the HOF also monotonically and almost linearly increased from 0.13 to 0.85. When the CNT density was converted to catalyst spacing, it spanned from 65 ± 5.5 to 6 ± 1 nm (1.4×10^{10} to 4.9×10^{11} catalyst/cm^2) (Figure 3). The underlying reason behind the relationship between alignment and density could be explained by a "crowding effect", as used in the carbon fibers field[26] and introduced by H. Dai to the describe the alignment of CNTs.[27] The crowding effect describes how neighboring CNTs physically interact with neighboring CNTs to determine the growth direction. Specifically, at low CNT density, the

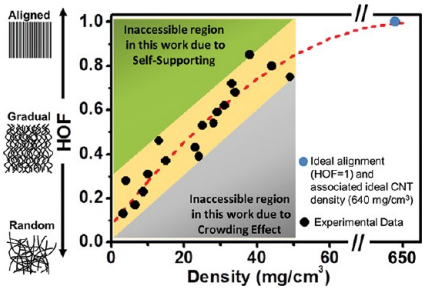

Figure 2. Graph of the alignment as a function of density showing the observed inseparable relationship between the alignment and density for few walled CNTs and the nearly linear relationship.

lateral confinement was nearly nonexistent which allowed the CNTs to experience minimal interaction with neighboring CNTs and allow them to proceed to grow in arbitrary directions away from the substrate. Under these conditions, the flexible, nonself-supporting CNTs created a nonaligned forest. In contrast, at high CNT density, the lateral confinement increased where the "crowding" of neighboring CNTs becomes significant, thus the CNTs could no longer grow in arbitrary directions but primarily in the vertical direction where the disturbance from neighboring CNTs was minimal. By including the ideal alignment (HOF = 1) and associated ideal CNT density (640 mg/cm^3), we

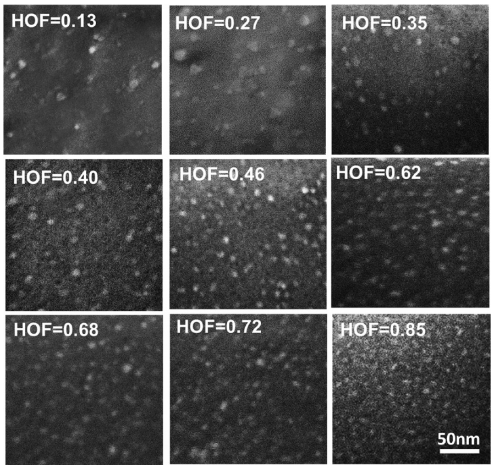

Figure 3. Observation of catalyst nanoparticles of the CNT forests with different degree of alignment by high resolution (300K×) scanning electron microscopy (SEM).

found that the relationship between HOF and CNT density was nonlinear and more specifically sigmoidal ("S-curve"). The sigmoid shape indicated that achieving perfect alignment through the crowding effect would become increasingly difficult as limiting mechanisms, such as imperfect spacing due to a finite diameter distribution, nonuniform growth rates, and vdWs adhesion between CNTs, begin to dominate the crowding process.

A qualitative explanation why all the experimental data in the HOF *versus* density plot fell along a narrow linear region with no points in the regions above and below could be described as follows. The lower region arose directly from the crowding effects where increased alignment occurred from increased CNT density, and therefore, at high density, low degree of alignment was inaccessible (crowding effect). The upper region arose from the nonself-supporting nature of the few-walled CNTs, that is, the ability of the CNTs to stand independently. Therefore, the CNTs formed a macroscopic structure by mutually supporting each other and could not align in high degree at low densities. This is different from large diameter (>10 nm) multiwalled carbon nanotubes (MWCNT) which can independently stand (self-supporting) at any density due to their higher flexural modulus.

To gain deeper insight of this continuous and restricted behavior, a simple quantitative model was constructed to explain the relationship between the alignment and CNT spacing. We chose the average spacing between CNTs as the fundamental parameter, although this cannot be directly estimated from the mass density as is the case for aligned CNTs. Therefore, we carried out a series of SEM observations of the substrates after CNT removal to estimate the average catalyst spacing, and assumed this was equal to the CNT spacing. The validity of this assumption was supported by the 84% catalyst activity reported for water-assisted CVD.[31]

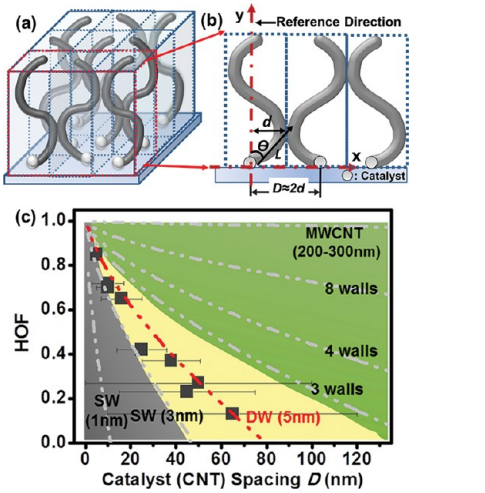

Figure 4. Modeling. (a) Schematic of the assumption to treat the CNT forest "many-body" problem to a more solvable "single-CNT" problem. (b) Graph of alignment as a function of catalyst (CNT) spacing to qualitatively explain how crowding effect dominates the alignment control in our work and how the degree of alignment and catalyst spacing can be controlled independently by tailoring the flexural modulus of the CNTs.

In this manner, we estimated the catalyst spacing (CNT spacing), and this was plotted versus HOF (Figure 4 and Supporting Information, Figure S2b). Similar to Figure 2, the HOF was strongly related to the catalyst spacing, whereas the HOF decreased with increased catalyst spacing. We developed a quantitative model to describe this behavior.

First, we assumed that the CNTs were confined to a volume defined by the catalyst spacing (D). This assumption allowed us to treat the CNT forest "many-body" problem as a more solvable "single-CNT" problem (Figure 4a). While for few-walled CNTs, the VdW interaction could signficant enough to increase stiffness of a bundle, as our model is a first order approximation, we neglect this factor. Second, we treated the CNT as an initially vertically oriented standing beam which is allowed to bend until it contacts the zone boundary. Classical mechanics describes the angular deviation from normal (ϕ) as: $\sin\theta \approx CD^{2/3}(E_{bend})^{-1/3}$, where D is catalyst spacing and E_{bend} is the flexural modulus, representing the CNT stiffness. Third, the HOF was calculated from this angular deviation according to $HOF \approx 1 - {}^{3}/_{2}\langle\sin\theta\rangle$. By this manner, we could quantitatively model the alignment of a forest using $HOF \approx 1 - [C(E_{bend})^{-1/3}]D^{2/3}$ with one fitting parameter, C, that includes geometrical factors (Supporting Information, Figure S4). We would like to emphasize that this relationship encapsulates all of the experimental trends observed in Figure 2 and Figure 4b. First, this relationship predicts that the CNT spacing and HOF should fall within a limited window as experimentally observed (Figure 2) given that the CNTs have a specific flexural modulus. Second, the model provides a quantitative description of the crowding effect where the

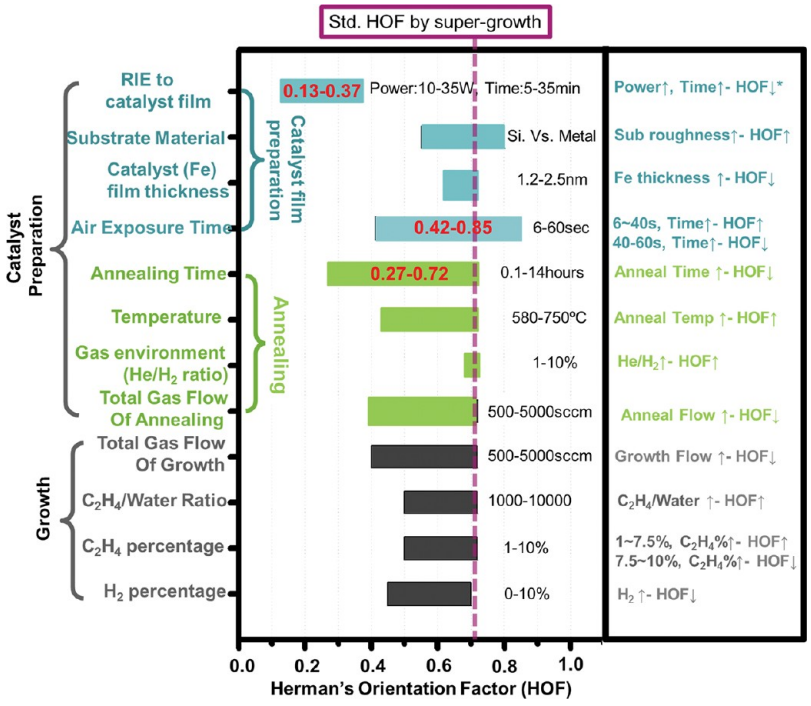

Figure 5. The effects of synthetic parameters on the degree of alignment.

alignment (HOF) is predicted to increase with decreases in the catalyst (CNT) spacing (D). The model was fitted and agreed well with experimental data (red dashed line, Figure. 3b), where C was found to be 4.42×10^8 and flexural modulus for 5 nm double-wall CNT (DWCNT) was ~503 GPa.

Our model could be expanded to describe the degree of alignment of arbitrary CNTs provided that the flexural modulus could be estimated. Here, the flexural modulus with different radius and wall numbers were calculated by

$$E_{\text{bend}} = E\frac{\pi}{4}[(R+\frac{h}{2})^4 - (R-\frac{h}{2})^4]$$

where R is the CNT radius, h is the wall thickness (h = wall number $\times$ 0.34 nm) and E is the CNT Young's modulus.[32] The flexural modulus was estimated for several CNT varieties, small and large diameter SWCNTs, and few-walled to many walled MWCNTs, and the relationship between the alignment (HOF) and CNT spacing was plotted (Figure 4b, gray dashed lines). As the flexural modulus increased with either increased diameter and/or wall-number, the accessible region shifted toward a higher degree of alignment. This model also showed that for more flexible CNTs (*i.e.*, smaller diameter and fewer walls) the dependence of alignment on catalyst (CNT) spacing became increasingly strong. For example, 1 nm SWCNTs would only exhibit random alignment if the catalyst spacing was less than ~7 nm. This would explain the difficulty to achieve aligned SWCNTs with small diameters. In contrast, it is predicted that a wall number of greater than eight would be sufficient to allow independent standing. The validity of our model was supported by good agreement of the predicted HOF (0.59) and experimentally observed HOF (0.62) for other experimental data, that is, standard water-assisted SWCNT forests with a diameter of 3 nm and spacing of 15 nm.[10] Although our model showed that the degree of alignment and catalyst spacing were tied and cannot be separated, it showed that the degree of alignment and catalyst spacing could be controlled independently by tailoring the flexural modulus of the CNTs.

Although the crowding effect elucidates a method to control the level of alignment, we investigated the effect of numerous synthetic parameters on the degree of alignment and found that a single synthetic parameter did not span the full range and demonstrated its own dependency and range of alignment control (Figure 5). All the detailed growth conditions to achieve the forests shown in Figure 1 are described in the Supporting Information, Table 1. The synthetic parameters investigated could be categorized simply as catalyst preparation and CNT growth. In general, the growth parameters demonstrated some level of control of alignment but the range was limited to 0.39 to 0.72, which represented typical values for CNT forests, and each of these approaches only reduced alignment from the standard level. As such, we concluded that alignment control though synthetic parameters was limited.

Conversely, the catalyst preparation parameters provided a wider range of alignment control (HOF of 0.13−0.85). This was understandable by considering the crowding effect as the CNT density is determined

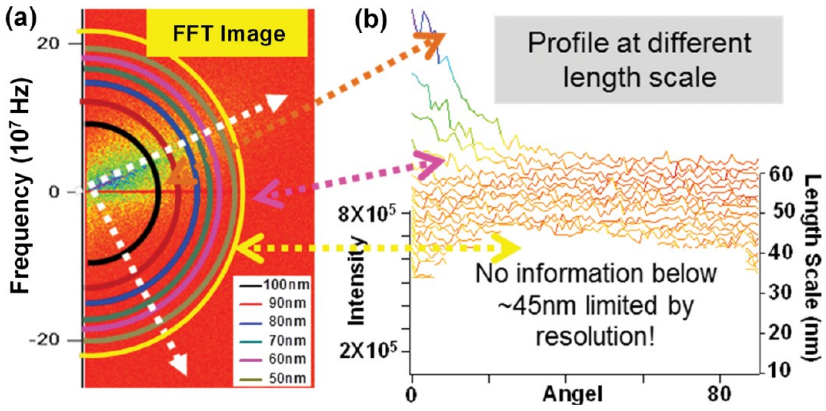

Figure 6. The procedure of alignment quantification: (a) Fast-Fourier transform (FFT) image based on crosssectional scanning electron microscope images; (b) sequential intensity profiles derived from FFT images at different length scales.

by the density of active catalysts, which was supported by the SEM observation (Supporting Information Figure S4 and Figure 4). Our catalyst consisted of sequentially sputtered Fe/Al_2O_3: 1.6−2.5 nm/40 nm on a silicon substrate, and the thin film was annealed at a high temperature in hydrogen (750 °C) to form nanoparticles. Among the various parameters studied, annealing time covered the widest range of controllable HOF from 0.27 to 0.72. The lower limit for the alignment could be further reduced to 0.13 by treating the catalyst film by reactive ion etching (RIE) after Fe deposition to further reduce the active catalyst sites. Although most of the growth parameters decreased HOF, only exposure to an ambient environment between the catalyst preparation (annealing) and growth stages provided a route to increase alignment as high as 0.85. We believe that the exposure to air following the annealing stage effectively increased the number of active catalysts by reducing aggregation.[23]

While certain growth conditions would expect to produce defective CNTs which could also affect alignment, the agreement of the experimental data with our simple model indicated that the flexural modulus was unchanged within our range of growth conditions. Defective CNTs would expect to exhibit a lower flexural modulus, and therefore show deviation from our model. Lastly, we briefly describe the estimation of the HOF based on the SEM observation. HOF is a commonly used parameter to characterize orientation and takes the value 1 for a system with perfect orientation parallel to a reference direction, and zero for completely nonoriented samples.[28] First, a two-dimensional fast Fourier transformation (FFT) intensity profile (Figure 6a) was calculated from a cross-sectional SEM image (Figure 1) (magnification: 10000×) of a forest from which the HOF was calculated by

$$f \equiv \frac{1}{2}(3\langle \cos^2 \phi \rangle - 1)$$
$$\langle \cos^2 \phi \rangle = \frac{\int_0^{\pi/2} I(\phi) \cos^2 \phi \sin \phi d\ \phi}{\int_0^{\pi/2} I(\phi) \sin \phi d\ \phi} \quad (1)$$

where ϕ was the angle between the structural unit vector and the reference direction, and $I(\phi)$ was the intensity profile of anisotropy as a function of ϕ from zero to $\pi/2$. For aligned CNTs, the intensity FFT image would have been oblong and anisotropic, and the structure unit vector referred to the long axis. The intensity profile $I(\phi)$ was then generated by mapping the intensity along an azimuth at a given radius (Figure 6b). The radius corresponds to a frequency in phase space and thus to a length scale in the real-space SEM image. For example, the length scale of 100 nm in the real-space corresponded to a frequency at 10^7 m^{-1}. We estimated the HOF by averaging six profiles corresponding to different real-space length scales from 50 to 100 nm with a resolution of 10 nm because this range roughly corresponds to the spacing between CNTs. The choice of this length scale was important to accurately represent the HOF. We note that our calculation of the degree of alignment (HOF) was based on the observation of CNT bundles at 10000× magnification by SEM as previously stated. Ideally, the HOF calculations should be performed for the individual CNTs; however, practically this would be nearly impossible by SEM. Previous HOF calculations were performed by TEM, and the HOF values did not change significantly compared to SEM. The alignment homogeneity throughout the CNT forests was investigated and was found to be unvarying throughout the forest with only minor variations at the very top (crust) and bottom (Supporting Information, Figure S5). Therefore, the degree of alignment of the middle section was chosen to represent the whole forest.

CONCLUSION

We proposed a general approach to control the degree of alignment of few-walled CNT forests synthesized on a substrate from nearly random to close to perfectly aligned (HOF: 0.13 to 0.85). Elucidating the relationship between the alignment and CNT mass density provided a route to control alignment by tailoring the active catalyst density. Many post processes, such as drawing and liquid induced densification, have

been developed to process CNT forests into sophisticated structures and forms, such as fibers and thin sheets, for high temperature actuators, CNT wafers for three-dimensional CNT-MEMS, highly packed bulk sheets for supercapacitors, and mildly compressed CNT forests as scaffolds for CNT–epoxy composites.[6] In these post processes, alignment has been recognized as a crucial factor that governs the processable structures, but in the past, the available varieties of alignment had been limited to two discrete states (aligned and nonaligned). Therefore, we expect that the wide variety of CNT forests with different alignments achieved in this work would open new opportunities for different structures and forms or new postprocesses. For example, we have found that the nonaligned forests show a higher ability for dry yarning, and thus it might provide a route to realize a yarnable single-walled carbon nanotube (SWCNT) material. From a different standpoint, by replacing the open space of the CNT forests with other materials, such as polymers,[29,30] we can envision the fabrication of CNT composites with differing CNT alignments.

EXPERIMENTAL METHODS

Synthesis. Carbon nanotube forests were synthesized from catalytic thin Al_2O_3 (~40 nm)/Fe (~1.6 nm) metal layers sputtered on Si substrates with an oxide layer (600 nm). Growth was carried out in a 1″ tube furnace by water-assisted chemical vapor deposition using ethylene carbon source (99.999%). Pure helium (99.9999%) and hydrogen (99.99999%) were used as carrier gases at 1 atm with a small and controlled amount of water vapor supplied from a water bubbler. The optimum water–carbon balance depended significantly on experimental conditions, such as growth temperature, ethylene flow rate, and catalysts.

Structure Observation. Scanning electron microscopy (SEM) images were taken using a Hitachi S-4800 instrument to observe the CNT alignment from the side-wall of forests. Transmission electron microscopy (TEM) JEOL JEM-2000FX was performed to observe the CNT diameter and wall number.

Conflict of Interest: The authors declare no competing financial interest.

Acknowledgment. Support by Technology Research Association for Single Wall Carbon Nanotubes (TASC) is acknowledged.

Supporting Information Available: Detailed synthesis conditions of CNT forests shown in Figure 1; TEM images of CNTs with different degree of alignment; the degree of alignment (HOF) plotted as a function of catalyst area density and catalyst (CNT) spacing; detailed explanation of modeling; SEM images of catalyst density on substrates as prepared by different catalyst preparation procedures; alignment homogeneity throughout the CNT forests checked by SEM and HOF calculation. This material is available free of charge *via* the Internet at http://pubs.acs.org.

REFERENCES AND NOTES

1. Rego, J. A.; Harvey, J. A. A.; MacKinnon, A. L.; Gatdula, E. Asymmetric Synthesis of a Highly Soluble `Trimeric' Analogue of the Chiral Nematic Liquid Crystal Twist Agent Merck S1011. *Cryst. Liq.* **2010**, *37*, 37–43.
2. Gutowski, T.; Dillon, T. G.; Stoller, S. Forming Aligned Fiber Composites into Complex Shapes. *CIRP Ann.: Manuf. Technol.* **1991**, *40*, 291–294.
3. Gupta, B. S.; Smith, D. K. Chapter X. Nonvowens in Absorbent Materials. *Text. Sci. Technol.* **2002**, *13*, 349–388.
4. Hennessey, W. J.; Spatorico, A. L. Stress-Induced Crystallization of Branched Polyethylene Terephthalate Films. *Polym. Eng. Sci.* **1979**, *19*, 462–467.
5. Koziol, K.; Vilatela, J.; Moisala, A.; Motta, M.; Cunniff, P.; Sennett, M.; Windle, A. High-Performance Carbon Nanotube Fiber. *Science* **2007**, *318*, 1892–1895.
6. Wardle, B. L.; Saito, D. S.; García, E. J.; Hart, A. J.; Guzmán de Villoria, R.; Verploegen, E. A. Fabrication and Characterization of Ultrahigh-Volume-Fraction Aligned Carbon Nanotube-Polymer Composites. *Adv. Mater.* **2008**, *20*, 2707–2714.
7. Endo, M.; Muramatsu, H.; Hayashi, T.; Kim, Y. A.; Terrones, M.; Dresselhaus, N. S. `Buckypaper' from Coaxial Nanotubes. *Nature* **2005**, *433*, 476.
8. Wu, Z. C.; Chen, Z. H.; Du, X.; Logan, J. M.; Sippel, J.; Nikolou, M.; Kamaras, K.; Reynolds, J. R.; Tanner, D. B.; Hebard, A. F.; *et al*. Transparent, Conductive Carbon Nanotube Films. *Science* **2004**, *305*, 1273–1276.
9. Gui, X.; Wei, J.; Wang, K.; Cao, A.; Zhu, H.; Jia, Y.; Shu, Q.; Wu, D. Carbon Nanotube Sponges. *Adv. Mater.* **2010**, *22*, 617–621.
10. Futaba, D. N.; Hata, K.; Yamada, T.; Hiraoka, T.; Hayamizu, Y.; Kakudate, Y.; Tanaike, O.; Hatori, H.; Yumura, M.; Iijima, S. Shape-Engineerable and Highly Densely Packed Single-Walled Carbon Nanotubes and Their Application as Super-Capacitor Electrodes. *Nat. Mater.* **2006**, *5*, 987–994.
11. Xu, M.; Futaba, D. N.; Yumura, M.; Hata, K. Tailoring Temperature Invariant Viscoelasticity of Carbon Nanotube Material. *Nano Lett.* **2011**, *11*, 3279–3284.
12. Duggal, R.; Hussain, F.; Pasquali, M. Self-Assembly of Single-Walled Carbon Nanotubes into a Sheet by Drop Drying. *Adv. Mater.* **2006**, *18*, 29–34.
13. Yamada, T.; Hayamizu, Y.; Yamamoto, Y.; Yomogida, Y.; Izadi-Najafabadi, A.; Futaba, D. N.; Hata, K. A Stretchable Carbon Nanotube Strain Sensor for Human-Motion Detection. *Nat. Nanotechnol.* **2011**, *6*, 296–301.
14. Kobashi, K.; Nishino, H.; Yamada, T.; Futaba, D. N.; Yumura, M.; Hata, K. Epoxy Composite Sheets with a Large Interfacial Area from a High Surface Area-Supplying Single-Walled Carbon Nanotube Scaffold Filler. *Carbon* **2011**, *49*, 5090–5098.
15. Awano, Y.; Sato, S.; Nihei, M.; Sakai, T.; Ohno, Y.; Mizutani, T. Carbon Nanotubes for VLSI: Interconnect and Transistor Applications. *Proc. IEEE* **2010**, *98*, 2015–2031.
16. Xu, M.; Futaba, D. N.; Yamada, T.; Yumura, M.; Hata, K. Carbon Nanotubes with Temperature Invariant Viscoelasticity from −196 to 1000 °C. *Science* **2010**, *330*, 1364–1368.
17. Hata, K.; Futaba, D. N.; Mizuno, K.; Namai, T.; Yumura, M.; Iijima, S. Water-Assisted Highly Efficient Synthesis of Impurity-Free Single-Walled Carbon Nanotubes. *Science* **2004**, *306*, 1362–1364.
18. Jiang, K.; Li, Q.; Fan, S. Nanotechnology: Spinning Continuous Carbon Nanotube Yarns. *Nature* **2002**, *419*, 801.
19. Zhang, X.; Jiang, K.; Feng, C.; Liu, P.; Zhang, L.; Kong, J.; Zhang, T.; Li, Q.; Fan, S. Spinning and Processing Continuous Yarns from 4-Inch Wafer Scale Super-Aligned Carbon Nanotube Arrays. *Adv. Mater.* **2006**, *18*, 1505–1510.
20. Zhang, M.; Fang, S. L.; Zakhidov, A. A.; Lee, S. B.; Aliev, A. E.; Williams, C. D.; Atkinson, K. R.; Baughman, R. H. Strong, Transparent, Multifunctional Carbon Nanotube Sheets. *Science* **2005**, *309*, 1215–1219.
21. Ci, L.; Punbusayakul, N.; Wei, J.; Vajtai, R.; Talapatra, S.; Ajayan, P. M. Multifunctional Macroarchitectures of Double-Walled Carbon Nanotube Fibers. *Adv. Mater.* **2007**, *19*, 1719–1723.
22. Patole, S. P.; Alegaonkar, P. S.; Shin, H. C.; Yoo, J. B. Alignment and Wall Control of Ultra Long Carbon Nanotubes in

Water Assisted Chemical Vapour Deposition. *J. Phys. D* **2008**, *41*, 155311–1—155311–6.
23. Esconjauregui, S.; Fouquet, M.; Bayer, B.; Robertson, J. Carbon Nanotube Growth: From Entanglement to Vertical Alignment. *Phys. Status Solidi B* **2010**, *247*, 2656–2659.
24. Klug, H.; Alexander, L. E. In *X-Ray Diffraction Procedures*; 2nd ed.; Wiley: New York, 1974.
25. Lovell, R.; Mitchell, G. R. Molecular Orientation Distribution Derived from an Arbitrary Reflection. *Acta Crystallogr.* **1981**, *A 37*, 135–137.
26. Merkulov, V. I.; Melechko, A. V.; Guillorn, M. A.; Lowndes, D. H.; Simpson, M. L. Alignment Mechanism of Carbon Nanofibers Produced by Plasma-Enhanced Chemical-Vapor Deposition. *Appl. Phys. Lett.* **2001**, *79*, 2970–2972.
27. Fan, S.; Chapline, M. G.; Franklin, N. R.; Tombler, T. W.; Cassell, A. M.; Dai, H. Self-Oriented Regular Arrays of Carbon Nanotubes and Their Field Emission Properties. *Science* **1999**, *283*, 512–514.
28. Gedde, U. W. In *Polymer Physics*; Kluwer Academic: Netherlands, 1995.
29. Gui, X.; Li, H.; Zhang, L.; Jia, Y.; Liu, L.; Li, Z.; Wei, J.; Wang, K.; Zhu, H.; Tang, Z.; *et al.* A Facile Route to Isotropic Conductive Nanocomposites by Direct Polymer Infiltration of Carbon Nanotube Sponges. *ACS Nano* **2011**, *5*, 4276–4283.
30. Ci, L.; Suhr, J.; Pushparaj, V.; Zhang, X.; Ajayan, P. M. Continuous Carbon Nanotube Reinforced Composites. *Nano Lett.* **2008**, *8*, 2762–2766.
31. Futaba, D. N.; Hata, K.; Namai, T.; Yamada, T.; Hiraoka, T.; Mizuno, K.; Hayamizu, Y.; Yumura, M.; Iijima, S. 84% Catalyst Activity of Water-Assisted Growth of Single Walled Carbon Nanotube Forest Characterization by a Statistical and Macroscopic Approach. *J. Phys. Chem. B* **2006**, *110*, 8035–8038.
32. Pantano, A.; Parks, D. M.; Boyce, M. C. Mechanics of Deformation of Single- and Multi-wall Carbon Nanotubes. *J. Mech. Phys. Solids* **2004**, *52*, 789–821.